

Photoluminescence properties of silica-based mesoporous materials similar to those of nanoscale silicon

Yu.D. Glinka^{1,2,a}, A.S. Zyubin^{1,3}, A.M. Mebel¹, S.H. Lin^{1,4}, L.P. Hwang^{1,4}, and Y.T. Chen^{1,4}¹ Institute of Atomic and Molecular Sciences, Academia Sinica, P.O. Box 23-166, Taipei 106, Taiwan, R.O.C.² Institute of Surface Chemistry of the National Academy of Sciences of Ukraine, prosp. Nauki 31, Kiev 252650, Ukraine³ Institute of Problems of Chemical Physics, Russian Academy of Sciences, Chernogolovka, Moscow Region 142432, Russia⁴ Department of Chemistry, National Taiwan University, Taipei 106, Taiwan, R.O.C.

Received 20 November 2000

Abstract. Photoluminescence (PL) from composites of 7- and 15-nm sized silica nanoparticles (SNs) and mesoporous silicas (MSs) induced by 266- (4.66-) and 532-nm (2.33-eV) laser light has been studied at room temperature. The multiband PL from MSs in the range of 1.0–2.1 eV is evidenced to originate from isolated bulk and surface non-bridging oxygens (NBOs) and from NBOs combined with variously placed 1-nm sized pore wall oxygen vacancies (OVs). The nature and diversity of NBO light-emitters are confirmed by *ab initio* calculations. The PL from SNs exhibits only a short wavelength part of the bands (1.5–2.1 eV) originated from isolated bulk and surface NBOs. This fact indicates that the highly OV-bearing structures occur only in extremely thin (~ 1 nm) silica layers. The similarity of spectroscopic properties of silica-based nanoscale materials to those of surface-oxidized silicon nanocrystals and porous silicon, containing silica-passivating layers of the same width, is discussed.

PACS. 78.55.-m Photoluminescence – 78.55.Mb Porous materials – 71.15.Mb Density functional theory, local density approximation, gradient and other corrections

1 Introduction

Recently discovered SiO₂-based mesoporous molecular sieves, which are usually called as mesoporous silicas (MSs), is a new type of material containing extremely thin silica fragments. It is known that the MS hexagonal pores of the size of several nanometers are arranged into a regular array with the wall thickness among pores of ~ 1 nm [1,2]. Owing to the great catalytic and adsorption properties of mesopores [1,2], their internal surface can be modified by semiconducting materials creating ordered semiconductor-insulator superlattices. Such kind of structures can find numerous applications in modern nanoscale semiconductor technology [3,4]. Also, because the passivating SiO₂ layers of ~ 1 nm width cover silicon nanoscales (nanocrystals, nanoscale fragments in porous silicon (PS)) [5–7], the MSs provide a unique opportunity to directly study the optical properties of ~ 1 -nm sized silica layers.

In this paper, we present the results of photoluminescence (PL) study of the composites of 7- and 15-nm silica nanoparticles (SNs) and MSs. The PL has been induced by harmonics of Nd:YAG (yttrium-aluminum-garnet) laser (266 and 532 nm) at room temperature. We show that the light-emitters are non-bridging oxygens (NBOs) situated both inside nanometer-sized bulk fragments and on

their surfaces. Based on *ab initio* calculations, numerous PL bands for MSs in the range of 1.0–2.1 eV are evidenced to originate from isolated bulk and surface NBOs and also from those combined with variously placed oxygen vacancies (OVs) in ~ 1 -nm sized pore walls. The OV-bearing silica structures occur exclusively in extremely thin (~ 1 nm) layers. Only isolated bulk and surface NBOs contribute to PL in the case of composites of 7- and 15-nm sized SNs supporting the conclusion made. Since the PL properties of silica nanoscale materials are found to be similar to those observed for silicon nanoscales [5–8], the experimental and theoretical finding presented here can be useful to clarify the origin of light-emitters in these materials.

2 Experimental section

We used two kinds of SNs (Aerosil, Degussa) with the nominal particle size of 7 and 15 nm (diameter). The synthesis of MSs, similar to that of originally proposed [1], was described earlier [9]. According to the X-ray diffraction patterns, the sample with d_{100} spacing of 3.83 nm (repeat distance - actually reflects the pore size, neglecting the wall thickness of ~ 1 nm) is characterized by crystalline ordering (MCM-41) [1,9], whereas those with d_{100} spacing of 2.9 and 7.1 nm are amorphous [9]. The powders have been pressed into pellets, then heat pretreated for 2 h

^a e-mail: yuri.d.glinka@vanderbilt.edu

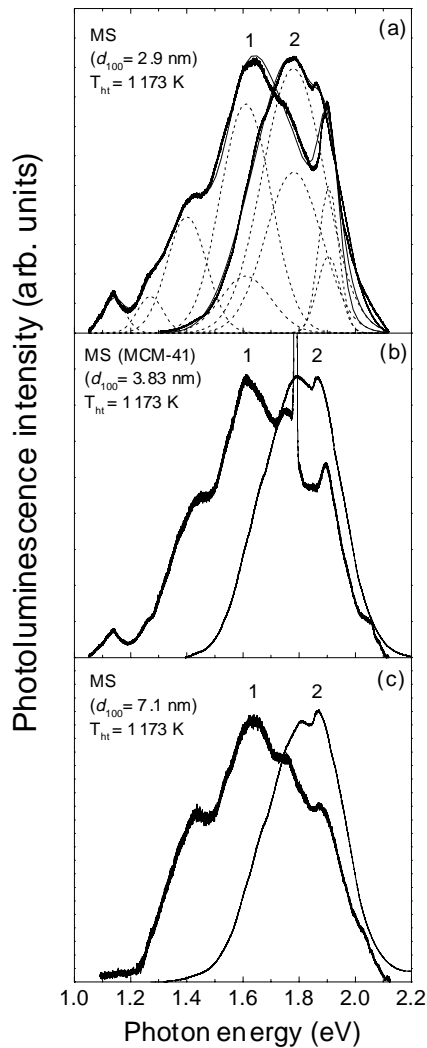


Fig. 1. Normalized PL spectra for MSs; $d_{100} = 2.9$ (a), 3.83 (b) and 7.1 nm (c); $T_{ht} = 1173$ K; $\lambda_{exc} = 532$ (1) and 266 nm (2). Dashed lines in (a) are the Gaussian profiles corresponding to different PL bands and thin lines show the accuracy of the spectral band deconvolution.

in air at $T_{ht} = 1173$ K. The PL was induced by Nd:YAG pulsed laser light (Spectra Physics, GCR-190) with a repetition rate of 30 Hz and $\lambda_{exc} = 266$ or 532 nm (8 ns) and measured at room temperature in air through a 0.5-m SpectraPro-500 monochromator (Acton Research Corporation) equipped by 1200 grooves/mm grating blazed for the 750 nm and cooled charge-coupled device (CCD) camera (Princeton Instruments, 330×1100 pixels). The spectra were measured within an accumulation time of 2 s.

3 Results and discussion

Figures 1(a)–(c) and 2(a)–(b) show the PL spectra measured with 532- (curves 1) and 266-nm light (curves 2) for MSs and SNs, respectively. The multiband PL in the range of 1.0–2.1 eV induced by 532-nm light from MSs is

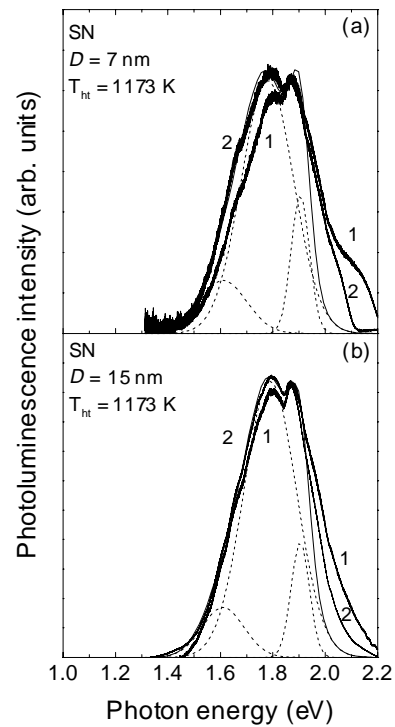


Fig. 2. Normalized PL spectra for SNs; $D = 7$ (a) and 15 nm (b); $T_{ht} = 1173$ K; $\lambda_{exc} = 532$ (1) and 266 nm (2). Dashed lines are the Gaussian profiles corresponding to different PL bands and thin lines show the accuracy of the spectral band deconvolution.

placed in the spectral range where the PL from surface-oxidized silicon nanocrystals [5,6], PS [8], hydrogenated amorphous silicon [10], Si-rich SiO_2 films [11] is typically observed. Only a short wavelength part of the compound multiband PL manifests itself under 266-nm excitation, indicating that only a part of the light-emitters relaxes radiatively in this case. By contrast, the spectra measured for SNs are similar for both excitations and contain only the short wavelength part. Totally, six components occur peaked at ~ 1.905 , ~ 1.78 , ~ 1.61 , ~ 1.40 , ~ 1.27 , and ~ 1.14 eV. The lifetime for the 1.905-eV light-emitters (8 and 15 μs at 300 and 90 K, respectively), in combination with the band position and its width, is typical for NBOs in bulk silica [12]. Accordingly, the 266- and 532-nm excitations used (4.66 and 2.33 eV) correspond to two NBO absorption bands peaked at 4.8 and 2.0 eV [12]. The remaining PL bands showed slower decay with a constant of 40–50 μs at 300 K and ~ 2 ms at 90 K, similar to nanoscale silicon [5,6,8]. The 1.905 and 1.78-eV bands were assigned to bulk and surface NBOs in our previous study of MSs [9] and SNs [13,14]. Curves 2 in Figs. 1(a)–(c) shows that the 1.905-eV band intensity as compared to 1.78-eV one increases with increasing the pore size of MS. This fact reflects the higher concentration of bulk NBOs with respect to the surface ones in larger pore sized MSs. We have suggested that all of the PL bands are originated from NBOs but they have different surrounding. Accordingly, the variation of the PL spectra in the range of 1.0–2.1 eV

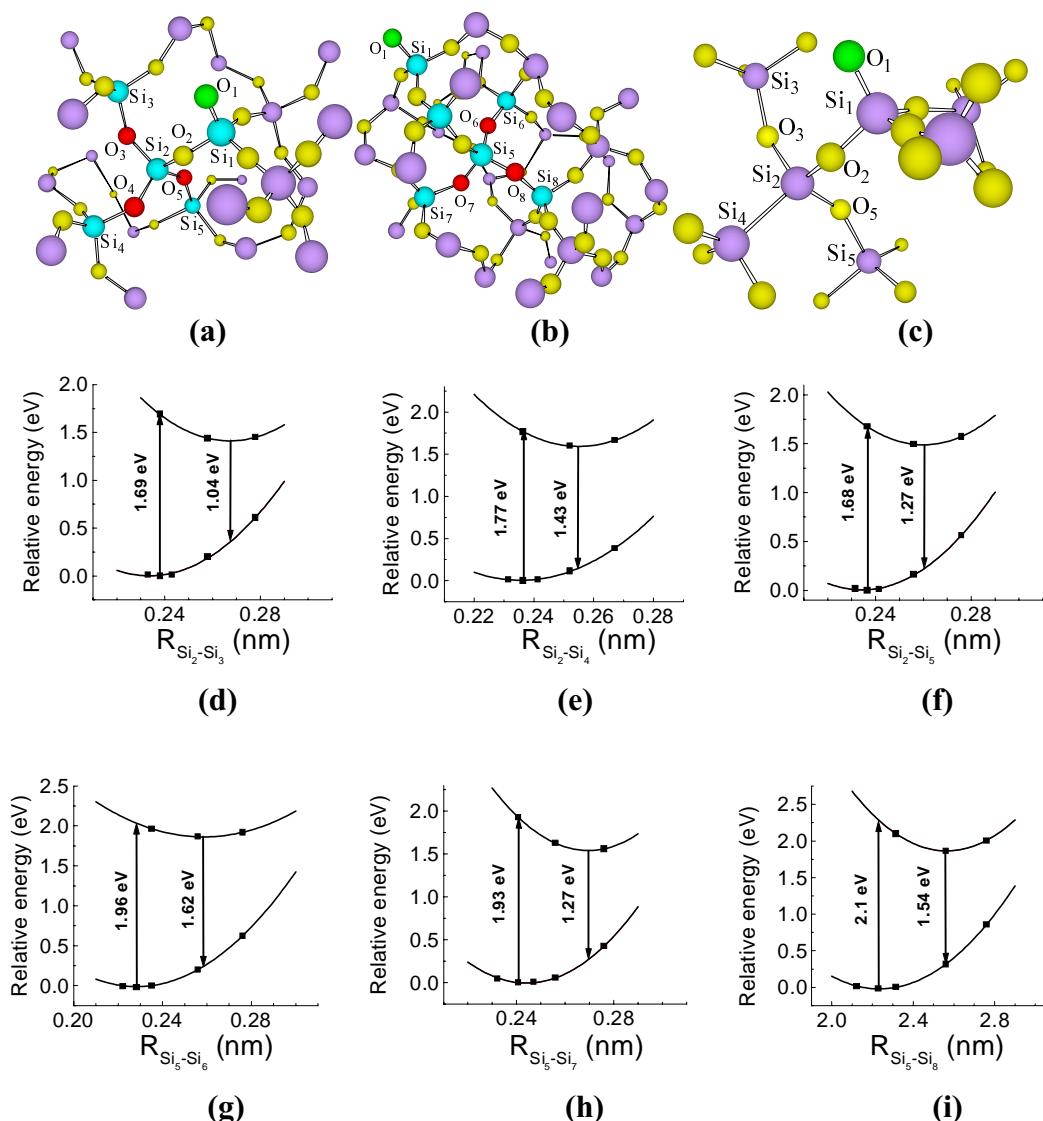


Fig. 3. The optimized geometry of α -quartz-like clusters used for modeling of NBO (O_1) combined with OVs situated in the second (a) and third (b) layers (O_3 - O_5 and O_6 - O_8 , respectively). Boundary hydrogens are not drawn. (c) The cluster used for TD-B3LYP calculations of vertical excitation and PL energies with OV situated at O_4 . (d) – (i) The parabolic fit of calculated points (■) for OVs situated at O_3 - O_8 sites. Arrows show excitation and PL transitions.

results from the redistribution of the concentrations of different light-emitter types. The thermal disruption of bulk and surface hydroxyls can be proposed as a mechanism of NBO formation [9,13–15]. Also, we assume that the heat pretreatment leads to oxygen and hydrogen release from MSs, giving rise to OVs inside pore walls [9,15]. Owing to the possible combination of bulk and surface NBOs with variously placed OVs, the energy of electronic transitions becomes lower, appearing as several red-shifted PL bands. Note that the sharp feature at 1.79-eV [Fig. 1(b)] is attributed to an uncontrolled impurity [11].

In order to test the aforementioned conclusion, we carried out *ab initio* calculations of SiO_2 clusters containing up to 60 heavy atoms, in which the NBO is surrounded by at least two Si-O layers [Figs. 3(a) and (b)]. The maximal cluster size is ~ 1 nm, similar to the wall thickness

in MSs. The geometry of clusters was optimized keeping the boundary Si atoms frozen at the crystal positions of α -quartz with their dangling bonds terminated by hydrogens. We used the ONIOM method [16] implemented in the GAUSSIAN-98 program [17], which allows us to treat the different layers of the clusters at different levels of theory. The inner layer was calculated at a high level (hybrid density functional B3LYP/6-31G* [18,19]) whereas the outer part was treated by the semi-empirical PM3 method [20]. The inner layer includes the NBO with nearest 5-9 Si and 12-15 O atoms. The applicability of this ONIOM (B3LYP/6-31G*:PM3) approach and the subdivision into two layers was tested by calculations of a model $\text{Si}(\text{OSiH}_3)_4$ cluster, where the inner layer was chosen as SiO_4 . The ONIOM optimized geometry showed a close agreement with B3LYP/6-31G*

results for the whole cluster and with the α -quartz lattice parameters. The ONIOM-optimized atomic coordinates were then applied to construct smaller clusters [Fig. 3(c)] designed for calculations of excited states. The excitation energies, E_{EXC} , were obtained using the time-dependent density functional theory (TD-B3LYP [21]) with a mixed basis set. We used the 6-31+G* basis set for NBO and 6-31G* for other atoms, except boundary Si's where the 6-31G basis set was applied. For the model cluster, $\text{OSi}(\text{OSiH}_3)_3$, the excitation energies calculated with such basis set are very close to those obtained with the full 6-31+G* basis set.

The computed vertical E_{EXC} for the electronic transition from the lone pairs (LP) of three nearest bridging oxygens to the singly occupied orbital of NBO, $E_{\text{EXC}}(\text{LP}\rightarrow\text{NBO})$, located in the OV-less clusters (1.9–2.0 eV) is close to the experimental value of 2.0 eV (Ref. [12]) and to the previous *ab initio* result for $\text{OSi}(\text{OSiH}_3)_3$, 2.18 eV, obtained by the multi-reference configuration interaction method [22]. Our calculations show that OVs are not likely to occur in the first layer; upon geometry optimization NBO inserts into them without barrier, restoring the Si-O-Si bridge. Alternatively, more remote OVs situated at O_3 , O_4 , and O_5 in the second layer [Fig. 3(a)] and O_6 , O_7 , and O_8 in the third layer [Fig. 3(b)] remain stable. According to the TD-B3LYP results, two low-lying excited states exist in OV-bearing clusters, one of which is similar to that for OV-less clusters (LP \rightarrow NBO) and another corresponds to the transition from the Si-Si bond to NBO (Si-Si \rightarrow NBO). A single OV in the second layer gives $E_{\text{EXC}}(\text{Si-Si}\rightarrow\text{NBO})$ in the range of 1.7–1.8 eV which are lower than $E_{\text{EXC}}(\text{LP}\rightarrow\text{NBO})$ varying from 2.1 to 2.2 eV. If OV appears in the third layer, the E_{EXC} for the two types of electronic states are comparable (1.93–2.10 eV for Si-Si \rightarrow NBO and 1.89–1.94 eV for LP \rightarrow NBO).

The PL energy, E_{PL} , can be estimated as the energy for a transition from the excited state at its equilibrium geometry to the ground state. For OV-less clusters the excited state geometry relaxation is small, resulting in a moderate Stokes shift ~ 0.1 eV [12] so $E_{\text{PL}}(\text{NBO}\rightarrow\text{LP})$ is only slightly lower than $E_{\text{EXC}}(\text{LP}\rightarrow\text{NBO})$. However, if the transition occurs from the Si-Si bond its length significantly changes; from 0.234 nm in the ground electronic state to 0.256–0.270 nm in the excited state. We scanned potential energy surfaces of the clusters along the Si-Si distance and fitted the calculated points by parabolas. Figures 3(d)–(i) shows this procedure for all OV positions considered. The $E_{\text{PL}}(\text{NBO}\rightarrow\text{Si-Si})$ values lie in the range of 1.04–1.62 eV. Two radiative channels in energy relaxation exist if an electron is excited to the singly occupied orbital of NBO: NBO \rightarrow LP and NBO \rightarrow Si-Si. The competition between these two channels can redistribute the intensities of the corresponding PL bands and shift the compound band as a whole.

The vertical energies should be assigned to bulk species because they were calculated for NBOs situated in undistorted SiO_4 tetrahedrons. On the other hand, it is reasonable to suggest that the surface NBOs are incorporated

into distorted tetrahedrons (twofold Si-O rings) [23]. The calculations show that the 1.78-eV PL band is consistent with such NBOs in OV-less clusters. If surface NBOs combine with variously placed pore wall OVs, the PL energies slightly vary as compared to the bulk species diversifying PL bands. Thus, the bulk and surface NBOs situated in OV-less and OV-bearing clusters give a set of PL bands covering the whole energy range of measured spectra.

4 Conclusions

In summary, we have shown that the PL from MS materials in the range of 1.0–2.1 eV is related to both isolated NBOs and those combined with variously placed pore wall OVs. Both bulk and surface species contribute to PL, additionally diversifying the PL spectra. The ~ 1 -nm sized walls among pores are found to be the defect-bearing SiO_2 structures. We state that the presence of such structures is the specific feature of extremely thin SiO_2 layers. Therefore, the spectroscopic properties of MS's are similar to those for surface-oxidized silicon nanocrystals and PS. The experimental and theoretical findings discussed in the current paper can help us to understand the nature of light-emitters in silicon nanoscale materials.

The authors acknowledge Academia Sinica and China Petroleum Corporation of Taiwan, Republic of China, for financial support. The work was supported by National Science Council of Taiwan: Y.D.G. and S.H.L. Grant No. 89-2113-M-001-050, A.M.M. Grant No. 89-2113-M-001-034, L.P.H. Grant No. 89-2113-M-002-033, and Y.T.C. Grant No. 89-2113-M-001-032.

References

1. C.T. Kresge, M.E. Leonowicz, W.J. Roth, J.C. Vartuli, J.S. Beck, *Nature* **359**, 710 (1995).
2. A. Monnier, F. Schuth, Q. Huo, D. Kumar, D. Margolese, R.S. Maxwell, G.D. Stucky, M. Krishnamurty, P. Petroff, A. Firouzi, M. Janicke, B.F. Chmelka, *Science* **261**, 1299 (1993).
3. Z.H. Lu, D.J. Lockwood, J.-M. Baribeau, *Nature* **378**, 258 (1995).
4. D.J. Lockwood, Z.H. Lu, J.-M. Baribeau, *Phys. Rev. Lett.* **96**, 539 (1996).
5. W.L. Wilson, P.F. Szajowski, L.E. Brus, *Science* **262**, 1242 (1993).
6. L.E. Brus, P.F. Szajowski, W.L. Wilson, T.D. Harris, S. Schuppler, P.H. Citrin, *J. Am. Chem. Soc.* **117**, 2915 (1995).
7. J.D. Holmes, K.P. Johnston, R.C. Doty, B.A. Korgel, *Science* **287**, 1471 (2000).
8. A.G. Cullis, L.T. Canham, P.D.J. Calcott, *J. Appl. Phys.* **82**, 909 (1997).
9. Yu.D. Glinka, S.H. Lin, L.-P. Hwang, Y.-T. Chen, *J. Phys. Chem. B* **104**, 8652 (2000).
10. T.M. Searle, in *Properties of Amorphous Silicon* (INSPEC, London, 1989), p. 369.

11. S. Hayashi, K. Yamamoto, *J. Luminesc.* **70**, 352 (1996).
12. L. Skuja, *J. Non-Cryst. Sol.* **179**, 51 (1994).
13. Yu.D. Glinka, S.H. Lin, Y.-T. Chen, *Appl. Phys. Lett.* **75**, 778 (1999).
14. Yu.D. Glinka, S.H. Lin, Y.-T. Chen, *Phys. Rev. B* **62**, 4733 (2000).
15. Yu.D. Glinka, M. Jaroniec, *J. Appl. Phys.* **82**, 3499 (1997).
16. I. Komaromi, S. Dapprich, K.S. Byun, K. Morokuma, M.J. Frisch, *J. Mol. Struct. (Theochem)* **461-462**, 1 (1999).
17. M.J. Frisch, G.W. Trucks, H.B. Schlegel, G.E. Scuseria, M.A. Robb, J.R. Cheeseman, V.G. Zakrzewski Jr, J.A. Montgomery, R.E. Stratmann, J.C. Burant, S. Dapprich, J.M. Millam, A.D. Daniels, K.N. Kudin, M.C. Strain, O. Farkas, J. Tomasi, V. Barone, M. Cossi, R. Cammi, B. Mennucci, C. Pomelli, C. Adamo, S. Clifford, J. Ochterski, G.A. Petersson, P.Y. Ayala, Q. Cui, K. Morokuma, D.K. Malick, A.D. Rabuck, K. Raghavachari, J.B. Foresman, J. Cioslowski, J.V. Ortiz, A.G. Baboul, B.B. Stefanov, G. Liu, A. Liashenko, P. Piskorz, I. Komaromi, R. Gomperts, R.L. Martin, D.J. Fox, T. Keith, M.A. Al-Laham, C.Y. Peng, A. Nanayakkara, C. Gonzalez, M. Challacombe, P.M.W. Gill, B. Johnson, W. Chen, M.W. Wong, J.L. Andres, M. Head-Gordon, E.S. Replogle, J.A. Pople, *Gaussian 98* (Revision A.7, Gaussian, Inc., Pittsburgh PA, 1998).
18. A.D. Becke, *J. Chem. Phys.* **98**, 5648 (1993).
19. C. Lee, W. Yang, R.G. Parr, *Phys. Rev. B* **37**, 785 (1988).
20. J.J.P. Stewart, *J. Comput. Chem.* **10**, 209 (1989).
21. M.E. Casida, C. Jamorski, K.C. Casida, D.R. Salahub, *J. Chem. Phys.* **108**, 4439 (1998).
22. G. Pacchioni, G. Ierano, *Phys. Rev. B* **57**, 818 (1998).
23. D. Ceresoli, M. Bernasconi, S. Iarlori, M. Parrinello, E. Tossatti, *Phys. Rev. Lett.* **84**, 3887 (2000).